Kai Mienert, Oksana Baer*, Claudiu Giusca and Andrea Prato

Parasitic load components for torque and force calibration: a Digital Twin concept

Parasitäre Lastkomponenten für die Drehmoment- und Kraftkalibrierung: ein Digitaler Zwilling Konzept

Abstract: The 5 MN m standard torque machine within the Competence Centre for Wind Energy (CCW) was developed at PTB. The Digital Twin (DT) of the torque transducer mounted inside the machine was developed to enable errors eliminations and resources optimization during operation. The machine can apply not only torque, but also bending moments and shear forces. At the same time, the DT concepts of force measurement devices and their application for static, continuous and dynamic calibrations was developed to improve calibration processes, preserve data quality and collect calibration data for improved decision making. In order to illustrate the functionality of both developed DT concepts, a study of parasitic load components in both devices is carried out using simulation with ANSYS and ABAQUS engineering software. The validation of the DT models was carried out using traceable measurements. The way to combine both concepts for comprehensive shading of the standard torque machine is discussed.

Keywords: calibration; data transfer; Digital Twin; finite element method; force transducer; torque transducer

Zusammenfassung: Die 5 MN·m Normalmesseinrichtung (NME) ist ein Bestandteil des Kompetenzzentrums für Windenergie (CCW) der PTB. Diese Drehmoment-NME kann neben reinem Drehmoment auch Biegemomente und Querkräfte aufbringen. Der Digitale Zwilling (DT) des in der Maschine verwendeten Drehmomentaufnehmers

wurde entwickelt, um den Einfluss von parasitären Lasten auf die Kalibrierung zu untersuchen und Optimierungen durchzuführen. Zeitgleich wurde die Anwendbarkeit von DT-Konzepten für Kraftaufnehmer in Bezug auf statische, kontinuierliche und dynamische Kalibrierungen zur Verbessrung des Kalibrierprozesses durch Steigerung der der Datenqualität der Kalibrierdaten für eine effektivere Entscheidungsfindung untersucht. Um die Funktionalität der beiden entwickelten DT-Konzepte zu veranschaulichen, wurde eine Studie zur parasitären Belastungskomponenten für beide Aufnehmer unter Verwendung von Simulationen mit ANSYS und ABAQUS Engineering Software durchgeführt. Die Validierung der DT-Modelle erfolgte durch rückführbare Messungen. Es wird diskutiert, welchen Beitrag beide Konzepte für die NME und die Kalibrierungen haben können.

Schlagwörter: Kalibrierung; Datenübermittlung; Digitaler Zwilling; Finite-Elemente-Methode; Kraftaufnehmer; Drehmomentaufnehmer

1 Introduction

Static calibration of uniaxial force and torque transducers is determined according to ISO 376:2011 [1] and EURAMET Calibration Guide [2]. The traceable calibration installations, deadweight or hydraulic systems, generate force components that are applied along the axis of symmetry of the transducers. However spurious force and moment components can be generated by a variety of causes, including the transducer not being perfectly aligned during assembly in the machine, the component being applied at an angle other than 0°, or the grasping and installation system of the transducer in the calibration machine itself generating spurious force and moment components. When such spurious components cannot be mechanically compensated, their effect to the sensors output shall be evaluated. Even if the misalignment value is nominally 0 mm or the angle of force application with respect to the axis of symmetry of the transducer is nominally 0°, both will have an uncertainty

---

*Corresponding author: Oksana Baer, Physikalisch-Technische Bundesanstalt, Department 1 Mechanics and Acoustics, Braunschweig, Germany, E-mail: oksana.baer@ptb.de. https://orcid.org/0000-0003-1612-0624
Kai Mienert, Physikalisch-Technische Bundesanstalt, Department 1 Mechanics and Acoustics, Braunschweig, Germany, E-mail: kai.mienert@ptb.de
Claudiu Giusca, Surface Engineering and Precision Centre, Cranfield University, Cranfield, UK, E-mail: c.giusca@cranfield.ac.uk
Andrea Prato, INRiM – National Institute of Metrological Research, Applied Engineering and Metrology, Turin, Italy, E-mail: a.prato@inrim.it. https://orcid.org/0000-0003-3733-4189

contribution that shall be accounted for [3]. Recently, an experimental study on different force transducers was performed and some sensitivity coefficients for different spurious side forces or bending moments were found [4]. These findings can be used to develop an advanced uncertainty budget model or to correct systematic effects.

In the view of creating DTs [5], typically addressed for Industry 4.0 applications, current work deals with the development of DTs for metrologichal applications of torque [6] and force [7] transfer standards. As a management and certification paradigm [8] which allows in real time to predict, optimise and maintain desired functionality of complex systems, a DT in manufacturing is a fit-for-purpose digital, or virtual, representation of an observable manufacturing element with synchronisation between the element and its digital representation [9].

The DT should be able to predict in real time the behavior of its physical representation with the precision and accuracy needed in each specific application [10]. The Industrial Digital Twin Association offers a detailed presentation and definition of a DT for Industry 4.0. It is the so-called Asset Administration Shell AAS [11]. DT on measurement systems is the part of this comprehensive definition.

Nevertheless, DTs in metrology have obligatory requirements to demonstrate measurement traceability. German National Metrology Institute PTB developed the following definition of the Digital Metrological Twin (DMT) [12]: a Digital Metrological Twin is a numerical (prediction) model that depicts a specific measurement process and indicates an associated measurement uncertainty for a specific measurement value, which is traceable to the units of the international. Moreover, it complies with the requirements that:

- the measurement uncertainty is calculated according to recognised standards [3];
- all input parameters are traceably determined and stated with the corresponding measurement uncertainty [3];
- and it is validated by traceable measurements.

Previous definition provides the requirements by fulfilment of which the generated DT output can be utilised for metrological services.

Simulation models, which are commonly used in the DT are listed here [13]. The DT models are divided into three main categories: physics-based models (Finite Element Method (FEM), structural health monitoring, computational inverse methods); data driven models (Machine Learning, digital signal processing, statistical inverse methods); surrogate models as a combination of both.

FEM is a popular technique used to model the transducer like measuring systems. For example, FE-modelling was used in [14] to ensure that the data, collected in a tensile experimental system, can be used quickly and efficiently to prove theoretical models and to determine required material properties. In [15] the FEM was used for the characterisation of a 5 MN m torque transducer. The FEM is implied to extend the calibration range up to 5 MN m. The method for determination of the Young's modulus is presented, and the defined value is used in FE-model. The simulated output signal deviates from the measured one by 17.5 %. Another simulation of a 4 kN m self-built torque transducer in MATLAB Simulink is reported in [16].

The 5 MN m standard torque machine [17] inside the Competence Center for Windenergie (CCW) at PTB is presented in Figure 1. The rendered picture shows how the transducer is mounted inside the machine. The machine can apply not only torque, but also bending moments and shear forces. The transfer standard is equipped with measuring bridges for measuring these quantities. The controlled multicomponent force application makes the standard torque machine unique worldwide. Also, the possibility to calibrate torque up to 5 MN m is unique. Such a comprehensive and unique functionality enables the generate calibration data on parasitic load components to validate DT.

The current work aims to represent the developed DT concepts for torque and force transducers in the Sections 2 and 3, respectively. The functionality of both developed DT concepts is tested with a study on parasitic loading components in both devices outlined in Sections 2.2 and 3.2. In Section 4 the main results of the work are discussed and finally in Section 5 the perspective on the future modelling of the standard torque machine is provided.

2 Torque transducer

In the following section the 5 MN m transfer standard of PTB and its DT are described. The multi step procedure to
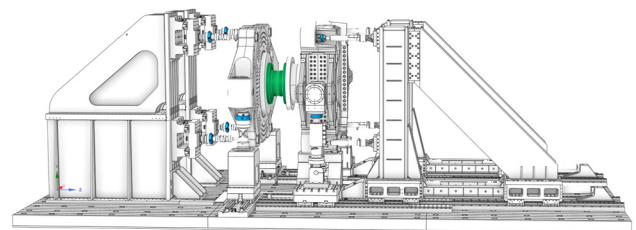

Figure 1: 5 MN m standard machine inside the Competence Center Windenergie (CCW) of PTB, 5 MN m transducer in the middle (green colored), force transducer of machine (blue colored).

create DT software is presented in details. To illustrate the DT functionality a use case study of model behaviour with parasitic loads is performed showing the effect of different combinations of loads on bridge output signal.

Figure 2 shows the 5 MN m transfer standard of PTB. The transfer standard is primarily designed to measure torque in the direction of the z-axis. This axis connects the two flanges. Overall, the transducer can measure forces and torques on the x-, y- and z-axis. For this purpose, the transducer has 8 measuring bridges consisting of strain gauges (SGs). The maximum nominal loads are listed in Table 1. The measuring bridges for M_z and F_z are redundant. The sensitivities of the individual bridges were taken from the manufacturer's data sheet. These do not replace calibration but provide a good estimation.

2.1 Digital Twin

The DT was built on the basis of the studies by Weidinger [15]. However, the methodology was adapted and extended according to the requirements of the current torque transducer DT concept. One task was to investigate the influence of parasitic loads on th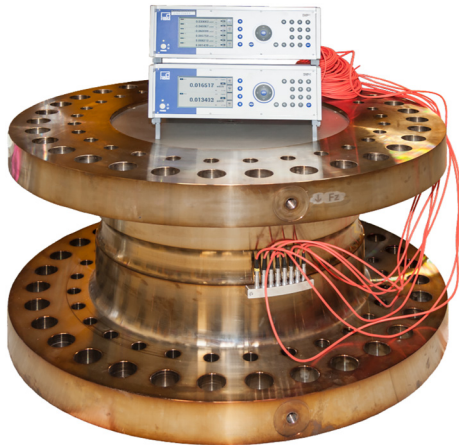e calibration. Furthermore, it will be investigated how DT methods can contribute to this. When calibrating a transducer, the torque must be applied as ideally as possible. Lateral forces or bending moments contribute to the measurement uncertainty. The sensitivity of the transducer to these influences depends on its design. Figure 3a shows the strain with an ideal and 3b with non-ideal torque application. The SGs are applied at the centre of the transducer. Shows how the strain changes when a force in F_x is applied in addition to the M_z torque. The effect on the strain of the strain gauges and consequently the output signal of the transducer is not defined. With a DT, the influence of parasitic forces and torques on the output signal could be predicted during calibration. The experiments to determine this with the real transducer would be very complex compared to a DT based experiment. For this reason, an FE-model was created from a 3D model of the transducer. Parameter studies were carried out on the FE model and a Reduced Order Model (ROM) was generated. The ROM was encapsulated in a software module to create a DT that could be used for experiments. These steps were realised and summarised as follows.

Step 1: Creation of a 3D model.

The 3D model was created using ANSYS Design Modeler. The information comes from the design drawings of the deformation body. When creating the 3D model, attention was paid to parametrisation. This makes it possible to determine the influence of manufacturing tolerances on the measured value and the position of the SGs. However, this is not part of this work. As Weidinger [15] shows, the

Figure 2: 5 MN m transfer standard of PTB with two DMP41 HBK strain Gauge amplifiers.
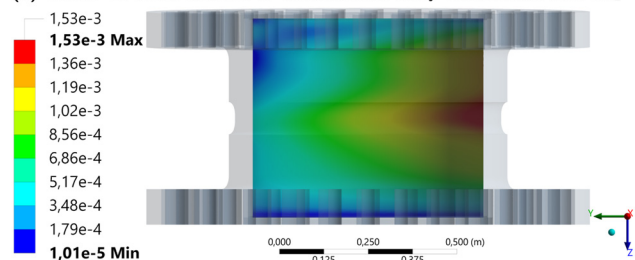
Table 1: 5 MN m transducer specifications.

Loadvector	Nominal load	Signal
Shear force F_x	3250 kN	0.73 mV/V
Shear force F_y	3250 kN	0.73 mV/V
Axial force F_z	4000 kN	0.23 mV/V
Bending torque M_x	1300 kN m	0.69 mV/V
Bending torque M_y	1300 kN m	0.69 mV/V
Torque M_z	5000 kN m	1.46 mV/V
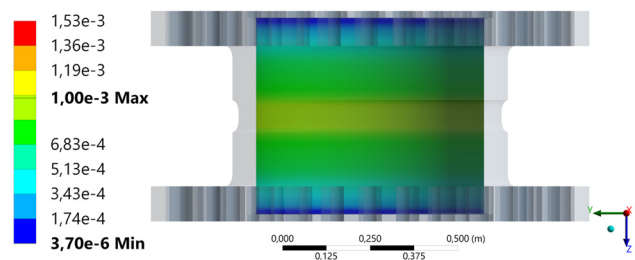
(a) Strain on inner surface of deformation body at nominal load M_z

(b) Strain on inner surface of deformation body at nominal load M_z and nominal load F_x

Figure 3: Elastic strain at (a) ideal load and (b) overlay of two loads.

SG consists of the "conductive lines", the "backend foil" and the "adhesive layer". Since 2017, new information has become available only on the geometry of the SG and the electrical characteristics. Unfortunately, this information is confidential to public. For the requirements of this DT, it was sufficient to model only the SG grids as surfaces on the deformation body. The Figure 4 shows the 3D model of the transducer.

Step 2: Finite Element Model.

Based on the 3D model from step 1, a FE-model was created in ANSYS Mechanical. The material properties of the deformation body were set according to [15]. The deformation body was meshed with approximately 2.7 million nodes. In the area of the SGs the mesh was refined to 1 mm. The grid size of the SGs ranged from 2 to 6 mm. The number of nodes in the overall mesh was increased until the strain no longer changed. The lower flange of the sensor was fixed and the forces and torques were applied to the upper flange via two remote points. The mean strain in the x-direction was determined over the area of the grids of the SGs. For example, the strain of a strain gauge at a M_z bridge was calculated as $7.496e^{-4}$ m/m at a torque of 5 MN m. All loads and the calculated strains were set as parameters. This allows design studies with different load configurations to be carried out in Step 3.

Step 3: Parameter studies and validation of finite element calculations.

Parameter studies were performed for the validation of the FE-model created in step 2. The already existing calibration certificates with torque in M_z direction for the measuring bridges M_{z1} and M_{z2} were used as reference. As forces and torques the calibration torques according to DIN 51309 [18] were chosen. The output signal of the bridge can be calculated from the equation (1) (see [15, 19]).

$$\frac{U_{\text{Out}}}{U_{\text{B}}} = \frac{1}{4} \cdot k \cdot (\epsilon_1 x - \epsilon_2 x + \epsilon_3 x - \epsilon_4 x) \tag{1}$$

Here U_{Out} is the output voltage of the measuring bridge, U_{B} is the supply voltage of the bridge, k is the SG factor,

ϵ_{nx} is the strain of the SG with the number n on the x-axis (coordinate systems Figure 4). However, the idealised calculation does not include any balancing resistors or parasitic resistors that may be used. Figure 5 includes these resistors $R_{\text{P1}}, R_{\text{P2}}, R_{\text{P3}}, R_{\text{P4}}, R_{\text{P5}}$ and R_{P6}. The voltage U_{Sense} is not considered further here. It is a 6-wire measurement setup but the cable and amplifier are set as ideal.

Due to the additional resistors, a new output bridge voltage $U_{\text{B}'}$ must be calculated with 2.

$$U_{\text{B}'} = U_{\text{B}} \cdot \frac{R_{\text{B}'}}{R_{\text{B}'} + R_{\text{P5}} + R_{\text{P6}}} \tag{2}$$

The resistances $R_{Z1}, R_{Z2}, R_{Z3}, R_{Z4}$ of the bridge branches are calculated from 3.

$$R_i = R_{\text{Pi}} + R_{\text{SGi}} \cdot (1 + k_{\text{SGi}} \cdot \epsilon_{ix}) \tag{3}$$

With 4 and 5, we get U_{Out}.

$$R_{\text{B}'} = \frac{(R_{Z1} + R_{Z2}) \cdot (R_{Z3} + R_{Z4})}{R_{Z1} + R_{Z2} + R_{Z3} + R_{Z4}} \tag{4}$$

$$U_{\text{Out}} = U_{\text{B}'} \cdot \left(\frac{R_{Z1}}{R_{Z1} + R_{Z2}} - \frac{R_{Z4}}{R_{Z3} + R_{Z4}} \right) \tag{5}$$

Figure 6 shows the calculated signal with the DT, the sensitivity from Table 1 and the calibration. For the torque steps shown in the figure, the FE model and the DT produce identical results. This is due to the fact that the DT is partly based on the FE model. Therefore, no values were plotted for the FE model. The calibration was performed on the 1.1 MN m torque standard machine at PTB. For calibration,

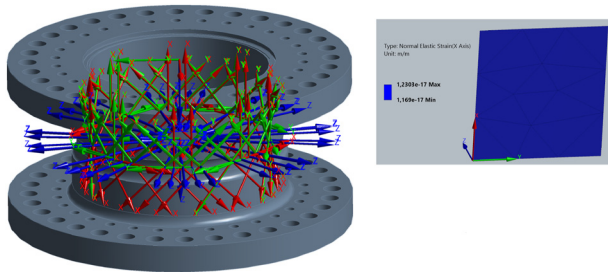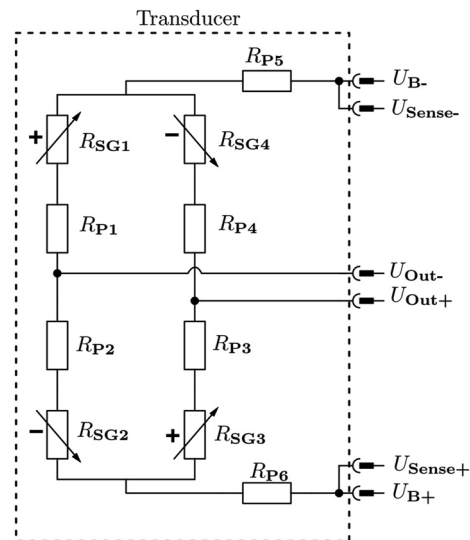**Figure 4:** 3D model of the transducer with coordinate systems of the SG grids, on the right SG grid as surface with coordinate system.

Figure 5: Extended wheatstone measuring bridge as a simplified model of the resistive properties of the measuring circuit within the 5 MN m transducer.
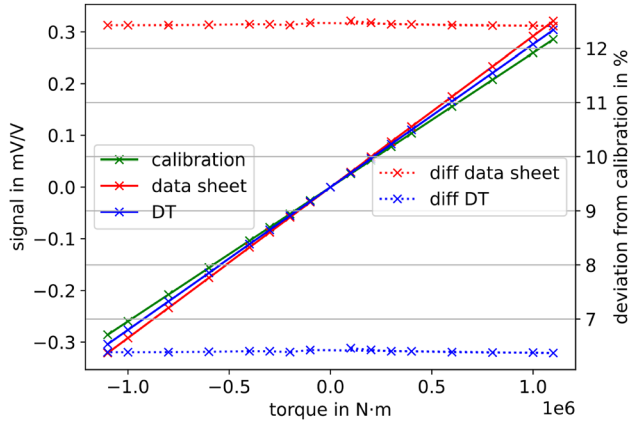
Figure 6: Comparison of the calibration according to DIN 51309; left legend: mV/V signal depending on torque; right legend: deviation from calibration depending on torque; partial range up to 1.1 MN m.

an expanded measurement uncertainty with $k = 2$ of 0.08 % applies.

Step 4: Reduced Order Model.

To integrate the behaviour of the FE-model into the DT, a Reduced Order Model (ROM) was created. The ROM is based on the Response Surface (RS) Method. In RS generation, RS is calculated for each output, which in this case is the average strain across SG mesh. For the calculation the input parameters $(F_x, F_y, F_z, M_x, M_y, M_z)$ are scattered. For this purpose, the ANSYS Design Explorer offers different methods such as Central Composite Design, Optimal Space-Filling Design, Box–Behnken Design, Sparse Grid Initialisation, Custom, Custom + Sampling and Latin Hypercube Sampling. For the transducer, Latin Hypercube Sampling was used to scatter the input parameters. In addition, the calibration torque steps for M_z were taken from the calibration certificates, which will be used later for validation. For the non-calibrated bridges, the forces and moments were set in 10 % increments from the maximum value. This gives a total of 178 design points. Genetic aggregation was chosen for the response surface calculation. The program uses the RS method Full 2nd-Order Polynomials, Non-Parametric Regression, Kriging and Moving Least Squares in parallel. In the end, the method with the least error is used. For further validation against the FE-model, 10 randomly generated design points have been used.

The ROM can then be exported as a Functional Mock-up Unit (FMU) according to the FMI standard [20]. To test the correct creation of the FMU, it was imported into ANSYS Twin Builder. The bridge signal in ANSYS Twin Builder was calculated with the equation (5) and compared with the results of the parameter studies.

Step 5: Digital Twin Software Implementation.

In this step, a software module was created with an API in Python, including the FMU. This allows the integration of additional functions. Another advantage is the possibility to run the DT during a calibration and compare the results in real time. The FMPy library from Dessault Systems [21] was used as a basis. This provides the ability to load and run an FMU. The following is a brief description of the parameters used in the library. The solver used is "CVODE" [22], the "start_values" are the forces and moments $F_x, F_y, F_z, M_x, M_y, M_z$. As this is a system without transient response, the following can be set: step_size = 1, start_time = 1, stop_time = 2. The unit is the second. The output is the strain of the 104 SG grids. Inside the FMU there is an XML file called "modelDescription.xml". This describes the interface of the FMU. FMPy uses the name of the corresponding output to select the required outputs. ANSYS only assigns a parameter number to the name, the rest is stored in the xml as a description. The units are also not stored in the field specified by the FMI standard and are stored under description during the generation of the FMU. For this reason, a mapping has been made between the parameter numbers of the outputs, the name of the output and the position in the array returned by FMPy with the outputs. This means that the possibilities of the FMI standard are not fully used.

For the calculation of U_{Out} from the strains of the SG grids, equation (5) was implemented in Python. For comparison with the real calibration results, the data from the calibration certificates were manually transferred to JSON files and stored in the module. With a DCC, this manual copying would be no longer necessary. A initial version of an good practice for torque according to DIN 51309 is currently being developed by PTB [23].

The current version of the DT provides the ability to compare actual readings with the model or another calibration during the measurement. The refresh rate has been set to 100 Hz. However, a graphical user interface has not yet been developed.

2.2 Model behavior with parasitic loads

The generated DT was used to investigate the behaviour of the transducer under parasitic loads. Figure 7 shows the result as a heatmap. All nominal values for the forces F_x, F_y, F_z and the torques M_x, M_y, M_z were applied as load cases. The heat map shows the response of each bridge in relation to the expected nominal value under ideal load.

The heatmap shows that the bridges M_{z1} and M_{z2} have a low sensitivity to parasitic loads. All other bridges are sensitive to at least one load. Bridges F_{z1} and F_{z2} have the highest sensitivity to parasitic loads. With such an analysis,
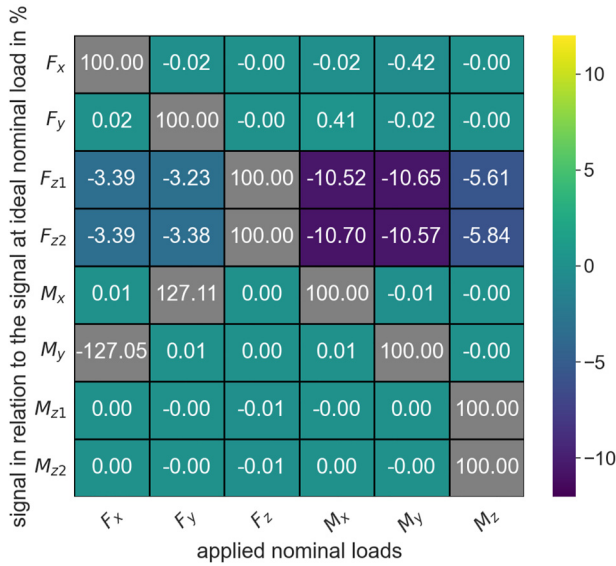
Figure 7: Crosstalk between measuring bridges at different combinations of loads.

the characteristics of a transducer can be better predicted. This can help in the assessment of systematic errors, for example. As this is a multi-component transducer, there is another advantage. Due to the crosstalk between the individual channels, it is not sufficient to use only one bridge. To determine all the resulting forces and moments, at least $F_x, F_y, F_{z1}, M_x, M_y, M_{z1}$ must be used.

3 Force transducer

To extend the applicability of the DT for metrological application described above, the following section deals with the application of the force transducer DT concept developed in [24] on the study of parasitic force components. To validate force transducer DT the main findings from experimental study of parasitic force components on commercial force transducer are given. The section deals with DT concept in short, focusing on the way to adjust the FE-model to capture non perfect force application. The resulting effect of sensitivity of force transducer on different load shift values is presented.

3.1 Experimental study of parasitic force components

At INRiM, the impact of parasitic components on the static calibration of uniaxial force transducers due to spurious side forces and bending moments was assessed [4]. These parasitic elements are typically caused by imperfect

verticality or alignment of the applied force. The objective was to deliberately create known side forces and bending moments by tilting and missaligning the transducer in relation to the vertical gravitational force during static calibration. This process was carried out on six different force transducers, and the resulting changes in calibration outcomes were analyzed. The aim was to derive sensitivity coefficients that can be utilised in the evaluation of uncertainty. To produce predetermined side forces and bending moments, INRiM force standard machines (FSMs), with a relative expanded uncertainty of 0.002 %, were equipped with hardened steel tilted plates, and the transducer being calibrated was placed between these plates while also being misaligned with respect to the center of the machine, which coincides with the axis of the applied vertical gravitational force. By adjusting the angle of tilt α or by shifting the transducer by a distance r in relation to the machine loading axis, the reference force produced by the FSM, can be broken down into vertical force, and side forces, or a bending moment, using simple trigonometrical formulas. Six different class 00 force transducers were tested in total.

Three sets of hardened steel (34CrNiMo6) tilted plates, with tilt angles of 1°, 2°, and 3°, were designed and manufactured. Each plate measures 200 mm × 200 mm × 70 mm and weighs approximately 30 kg. The plate dimensions and tilt angles were chosen to ensure that they fit the load platform of the machines and maintain system stability under high loads, accounting for steel-to-steel friction between the tilted plate and a typical transducer. Three misalignments, without tilted plates, are applied to the transducers to create a pure bending moment, with values of 2 mm, 4 mm, and 6 mm. For each tilt angle α (including 0°) or misalignment r, the transducers are rotated around their axis with 45° intervals, and three loads (10 %, 50 %, and 100 % of the transducer's capacity) were applied. In total, 168 deflection measurements (4 tilt angles × 8 rotations × 3 loads + 3 misalignments × 8 rotations × 3 loads) are performed for each transducer. The sensitivity S in (mV/V)/kN was calculated for each condition, taking into account the tilt angle to ideally compensate for its influence. Results showed that different tilted plates generating spurious side forces mostly follow a sinusoidal trend, with increasing amplitude at higher tilt angles α (or higher side force), resulting in increased standard deviation (Figure 8).

On the other hand, it was found that different misalignments r creating spurious bending moments exhibited no sinusoidal trend and small standard deviations in sensitivity for different rotations Figure 9. On the contrary, when performing the mean sensitivity value from the eight rotations under various load conditions, it was found that
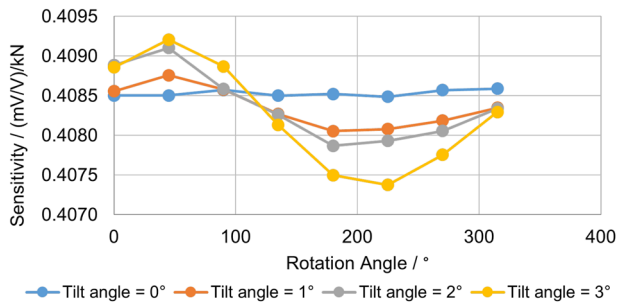
Figure 8: Sensitivity of the 5 kN transducer as function of the rotation angle with different spurious side force (or tilt angles) at an applied vertical force of 2.5 kN [4].

it changed as the spurious side forces or bending moments increase. However, the magnitude of mean sensitivity variations due to side forces in Figure 8 was much smaller than the one due to bending moments in Figure 9.

3.2 Digital Twin study of parasitic force components

The developed concept of force measurement device DMT covers three main functions [24].
– DMT allows for a prompt reading of selected device information, e.g. sensors reading (temperature, strain sensors). Here the key role plays the speed of communication as well as maintaining data quality. The physical-to-virtual communication is realised by reading of relevant device information from a DCC for force measurement.
– The second function of DT is the data processing by means of FEM. The main outcome of data processing is the prediction of force measurements device output signal as well as measurement uncertainty. For the DMT it is crucial that the input/output parameters
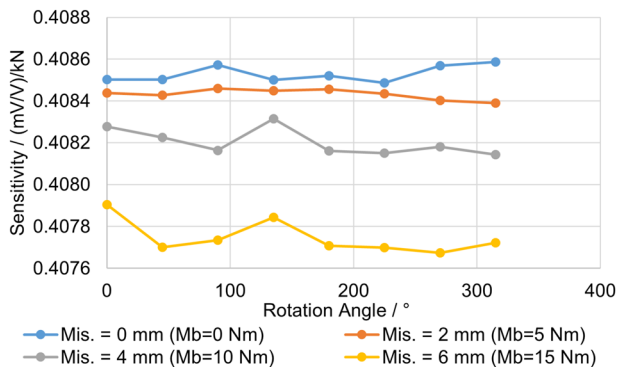
are traceable and are stated with the corresponding measurement uncertainty. Additionally, the validation of calibration models within DT must be performed using traceable measurements. In the current work the digital construct based on FEM contributing towards DMT of force measurement device was developed.
– The third function enables saving of the modelled output which can be used to recalculate uncertainty in future calibration procedures. The synchronisation between the force measurement device and its DT is performed after each calibration process in form of reading and subsequent update of the DCC by means of Python programming. The calculated with DT device output as well as measurement uncertainty are saved after each calibration in a database, representing the device history.

3.2.1 Model setup

Geometrical model of the force transducer used for static calibration is described in details in [24]. Experimental study, described in Section 3.1, investigated the behaviour of the commercial force transducer mounted between two tilted plates under compression. Due to confidentiality reasons no information about bridge wiring of the commercial force transducer as well as the precise geometry of the loading cell is available. This is a common restriction which makes creation of the DT challenging. To overcome this, the digital construct developed in [24] was studied, where the geometry as well as bridge wiring was custom made and with this well known, see Figure 10.

To simulate eccentric axial loading, which generate parasitic force components, an additional geometrical body was introduced to the assembly, see Figure 11. A ring element was modelled to mimic round mass elements and was
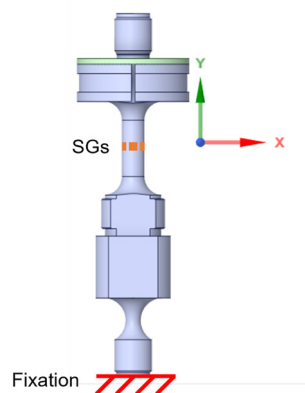

Figure 9: Sensitivity of the 5 kN transducer as function of the rotation angle with different spurious side force (or tilt angles) at an applied vertical force of 2.5 kN [4].

Figure 10: Geometrical model of the force transducer, showing SGs positions as well as fixation boundary condition.

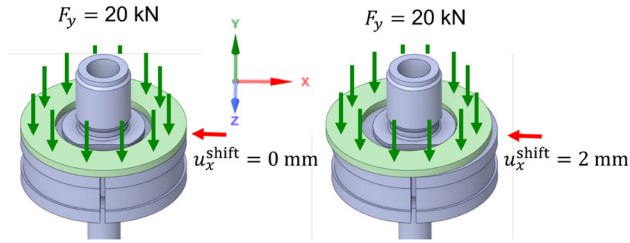**Figure 11:** Force transducer model, showing ring element shift and applied force.

Figure 12: Diagram of axial strain distribution in deformed force transducer (scale factor 10), loaded to 20 kN and 2 mm shift.

Figure 13: Sensitivity of the 20 kN force transducer as function of the axial position at applied nominal force of 20 kN at various shift values.

attached above. The concentrated axial force F_y was applied on the upper surface of the ring element, see Figure 11. By shifting the ring in x direction an eccentric load was introduced. The simulated shift values u_x^{shift} are 1, 2 and 3 mm.

According to the methodology described in [25], spatial displacements and associated positions of a set of 36 × 31 (1116) surface nodes at the centre of the transducer, see Figure 10, were collected from FE-model and subsequently used to calculate longitudinal and transversal strain between these surface nodes, and the equivalent mV/V output signal. In here, the equivalent mV/V output signal was calculated by averaging the data extracted from adjacent surface nodes to correspond to the output of a SG of a 2 mm by 2 mm surface area.

3.2.2 FE-analysis results

Steady state static analysis of ABAQUS software was used to calculate loading of the force transducer to 20 kN maximum nominal force. The deformed shape of the force transducer is presented in Figure 12. The scale factor 10 was used for better visualisation.

Figures 13 and 14 present a plot of the mean sensitivity as a function of axial position and the sensitivity as a function of the radial position in the middle of the transducer (15 mm axial position), respectively. An axial variation in mean sensitivity of approximately 2 % was already expected in the central area of interest of the transducer [25], however, the simulations predict that, during eccentric loading, the mean mV/V output of the sensors will depart unevenly axially from conformal loading output, as indicated by the bat-wing shape of the mean sensitivity errors in the middle part of the transducer in Figure 13. At each axial position, the absolute sensitivity difference between the eccentric and conformal loading is proportional with the amount of load-
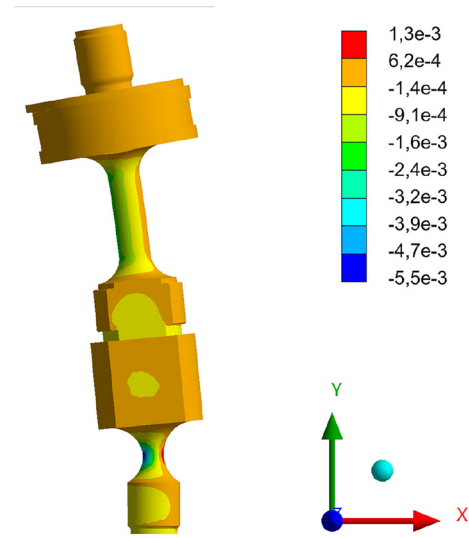
ing weight shift, approximately 0.06 %/mm in the middle of the transducer, see Figure 14.

The FE-model implementation presented in this paper allows the top end of the transducer to move free, however, this is probably not the case during the practical use of the force sensor. Nevertheless, the results indicate that systematic errors in the force sensor output are expected with eccentric loading, even with a configuration of the strain sensors that reduces bending effects.
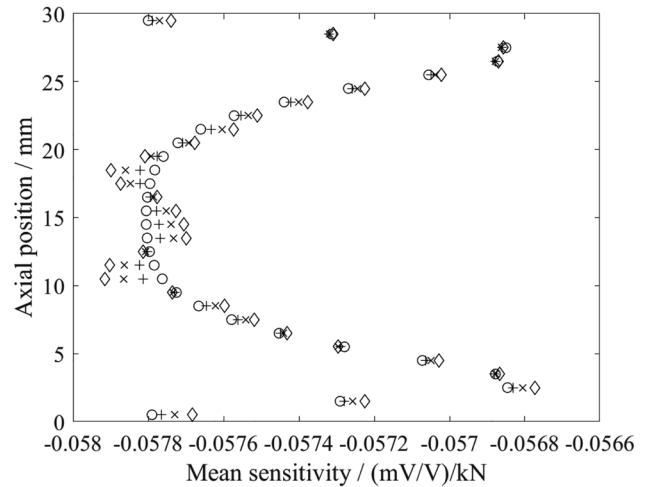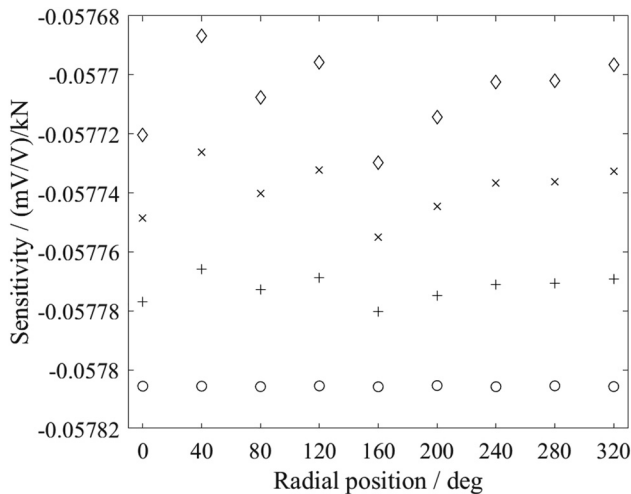
Figure 14: Sensitivity of the 20 kN force transducer as function of the radial position at applied nominal force of 20 kN at various shift values.

4 Discussion

Two FEM-based digital constructs were developed considering the requirements for further application in the field of metrology. The application of the DT approach for the study of parasitic loading component during static torque and force calibration showed promising results in terms of qualitative modelling of effects taking place during calibration. This is due to physical nature of the FEM accounting for specific geometry of the object, material properties and boundary conditions. The applicability of the FEM based DT of force transducer was limited by the restricted availability of the drawings of the commercial sensors as well as bridge wiring. As a solution, the corresponding sensors should be replaced by a black box model, which in its turn increases the uncertainty.

Another challenge consists in the necessity to validate the DT model with the traceable measurements. In the case of calibration modelling it is quite challenging to introduce known parasitic loading component in the calibration machine since it is from one hand designed to compensate transversal components and from the other hand is sensitive to mounting conditions and representation of the tilted plates can lead to machine collapse.

DTs of measuring devices are able to contribute to the issue of correcting systematic error related to parasitic loads. From such correction in the future one can derive the way for improved measurement uncertainty calculation considering parasitic force component effect.

Uncertainty of input data as well as effect of its processing in DT environment must be evaluated. A comprehensive review on data uncertainty in DT is given in [26]. In the

force transducer model the following sources of uncertainty affects the final calculated output signal and its uncertainty: geometrical data, input data from DCC, material properties data, uncertainty of FEM, uncertainty of FE-model implementation, uncertainty of data transfer from digital construct to physical object and vice versa, etc.

5 Conclusions and outlook

Within the current research, digital constructs for torque and force transfer standards were developed with the goal of further applications in DMT. Despite different approaches for data communication, there are similarities which will allow in the future to use both digital constructs in the comprehensive DT representation of the entire machine. The key role in such implementation plays the use of a Digital Calibration Certificate as the source of input parameters as well as a way to improve measurement uncertainty.

The use case study on the parasitic components influence on the calibration results shows that both FE-models are able to represent the qualitative effect of the force application shift on the output result of transfer standards but it still has insufficient precision to make an improvement of the measurement uncertainty.

Conflict of interest statement: The authors declare no conflicts of interest regarding this article.

References

[1] ISO 376:2011, *Metallic Materials — Calibration of Force-Proving Instruments Used for the Verification of Uniaxial Testing Machines*, International Organization for Standardization, 2011.

[2] *"Guidelines on the Calibration of Static Torque Measuring Devices. Version 2.0, The EURAMET Technical Committee for Mass and Related Quantities*, 2011.

[3] Joint Committee for Guides in Metrology, "JCGM 100: evaluation of measurement data — guide to the expression of uncertainty in measurement," JCGM, Tech. rep., 2008.

[4] A. Prato, E. Giacardi, A. Facello, F. Mazzoleni, A. Germak, et al., "Influence of parasitic components in the static calibration of

uniaxial force transducers," in *Proceedings IMEKO 24th TC3, 14th TC5, 6th TC16 and 5th TC22 International Conference*, 2022.

[5] K. Y. H. Lim, P. Zheng, and C.-H. Chen, "A state-of-the-art survey of Digital Twin: techniques, engineering product lifecycle management and business innovation perspectives," *J. Intell. Manuf.*, vol. 31, no. 6, pp. 1313−1337, 2020.

[6] Physikalisch-Technische Bundesanstalt, *GEMIMEG-II*. Available at: https://www.gemimeg.ptb.de/gemimeg-startseite/ [accessed: Mar. 19, 2023].

[7] Physikalisch-Technische Bundesanstalt, *ComTraForce*. Available at: https://www.ptb.de/empir2019/comtraforce/home/ [accessed: Mar. 19, 2023].

[8] D. Stargel and E. Glaessgen, "The digital twin paradigm for future NASA and U.S. Air force vehicles," in *53rd AIAA/ASME/ASCE/AHS/ASC Structures, Structural Dynamics and Materials Conference*, 2012.

[9] ISO 23247-1:2021, *Automation Systems and Integration — Digital Twin Framework for Manufacturing — Part 1: Overview And General Principles*, International Organization for Standardization, 2021.

[10] L. Wright and D. Stuart, "How to tell the difference between a model and a digital twin," *Adv. Model. Simul. Eng. Sci.*, vol. 7, no. 13, pp. 1−13, 2020.

[11] Industrial Digital Twin Association e. V., *IDTA — Der Standard für den Digitalen Zwilling*. Available at: https://industrialdigitaltwin .org/technologie [accessed: Mar. 19, 2023].

[12] F. Härtig, *VirtMet Applications and Overview*, Berlin, 2021. https:// www.ptb.de/cms/fileadmin/internet/PSt/pst1/VirtMet2021/ VirtMet2021_Programme_v5.pdf

[13] Industrial Digital Twin Association e. V., *IDTA 02005-1-0 Provision of Simulation Models*, Frankfurt am Main, Imprint, 2022.

[14] D. Antók, T. Fekete, L. Tatár, P. Bereczki, E. Kocsó, "Evaluation framework for tensile measurements, based on full-field deformation measurements and digital twins," *Procedia Struct. Integr.*, vol. 37, pp. 796−803, 2022.

[15] P. Weidinger, C. Schlegel, G. Foyer, and R. Kumme, "D6.2 — characterisation of a 5 MN m torque transducer by combining traditional calibration and finite element method simulations," in *Proceedings Sensor 2017*, Wunstorf, Germany, AMA Service GmbH, Von-Münchhausen-Str. 49, 31515, 2017, pp. 516−521.

[16] S. Kock, G. Jacobs, D. Bosse, and F. Strangfeld, "Simulation method for the characterisation of the torque transducers in MN m range," *J. Phys.: Conf. Ser.*, vol. 1065, no. 4, p. 042014, 2018.

[17] C. Schlegel, H. Kahmann, P. Weidinger, R. Kumme, "New perspectives for MN m torque measurement at PTB," in *IMEKO 23rd TC3, 13th TC5 and 4th TC22 International Conference*, 2017.

[18] DIN 51309, *Werkstoffprüfmaschinen_- Kalibrierung von Drehmomentmessgeräten für statische Drehmomente*, Berlin, Beuth Verlag GmbH Berlin, 2022.

[19] HBK (Hottinger, Brüel & Kjær), *The Wheatstone Bridge Circuit*. Available at: https://www.hbm.com/en/7163/wheatstone-bridge-circuit/ [accessed: Mar. 19, 2023].

[20] Modelica Association, *FMI Functional Mock-Up Interface*, 2023. Available at: https://fmi-standard.org/.

[21] Dassault Systemes, *FMPy*. Available at: https://github.com/CATIA-Systems/FMPy [accessed: Mar. 19, 2023].

[22] Lawrence Livermore National Security and Southern Methodist University, *Sundials Documentation*. Available at: http://www .sheffieldsolarfarm.group.shef.ac.uk/solar-panel-data [accessed: Mar. 19, 2023].

[23] Digital Calibration Certificate, *ComTraForce*. Available at: https:// www.ptb.de/dcc/ [accessed: May. 31, 2023].

[24] C. Giusca, O. Baer, C. G. Izquierdo, S. G. Molto, A. Prato, *Validation Report for the Digital Twin Software, Considering Requirements of Digitisation and Industry 4.0, for Static, Continuous and Dynamic Force Transfer Standards Including Measurement Uncertainty Determination*. Cranfield, CERN, Version 1.0, 2022.

[25] C. L. Giusca, O. Baer, C. G. Izquierdo, S. L. Molto, A. Prato, et al., "Digital representation of a load cell," in *Proceedings of TC3 Conference 2022*, 2022.

[26] J. Ríos, G. Staudter, M. Weber, R. Anderl, and A. Bernard, "Uncertainty of data and the digital twin: a review," *Int. J. Prod. Lifecycle Manag.*, vol. 12, no. 4, pp. 329−358, 2020.

Bionotes

Kai Mienert
Physikalisch-Technische Bundesanstalt,
Department 1 Mechanics and Acoustics,
Braunschweig, Germany
kai.mienert@ptb.de

Kai Mienert has been working at the Physikalisch-Technische Bundesanstalt since September 2020. He works as a scientist in the GEMIMEG-II project and is a graduate engineer in automation technology and electrical engineering. His focus is on automation of industrial processes, embedded systems. In GEMIMEG-II he works on the investigation of the applicability of Digital Twins in metrology and partly on the development of the DCC.

Oksana Baer
Physikalisch-Technische Bundesanstalt,
Department 1 Mechanics and Acoustics,
Braunschweig, Germany
oksana.baer@ptb.de

Oksana Baer has been a member of the Physikalisch-Technische Bundesanstalt (PTB) in Germany since January 2021. Oksana Baer obtained her PhD in the field of Mechanical Engineering with the focus on micromechanical creep damage modelling. As member of the SmartCom project team at PTB, she primarily took an active part in the development of the "DCC" Best Practice examples. Another research focus lies on force calibration, digitalisation in metrology as well as modelling of manufacturing processes and material properties.

Claudiu Giusca
Surface Engineering and Precision Centre,
Cranfield University, Cranfield, UK
c.giusca@cranfield.ac.uk

Andrea Prato
INRiM — National Institute of Metrological
Research, Applied Engineering and
Metrology, Turin, Italy
a.prato@inrim.it

Claudiu Giusca is Senior Lecturer at Surface Engineering and Precision Centre of Cranfield University. Dr. Giusca expertise is in the metrology associated with the use of optical surface topography measuring instruments, surface texture and micro-coordinate measurements and analysis, X-ray computed tomography, design and build of primary instrumentation. Previous to Cranfield University, Dr. Giusca was the lead scientist in Dimensional Surface Metrology group at National Physical Laboratory, the UK's national metrology institute.

Andrea Prato is a researcher at the National Institute of Metrological Research (INRIM, Italy), within the Applied Metrology and Engineering Division. Andrea Prato obtained his PhD in Metrology and MSc degree in Physics, his main metrological research areas are Force, Hardness, Gravimetry, Vibrations, Acoustics and mechanical properties of materials.